Pergamon

Materials Research Bulletin, Vol. 33, No. 10, pp. 1503–1515, 1998

0025-5408/98 $19.00 + .00

PII S0025-5408(98)00144-5

SOME GEOMETRICAL SINGULARITIES IN THE CHARACTERIZATION OF VAPOR GROWN CARBON FIBERS USING LASER DIFFRACTION TECHNIQUE

A. Madroñero[1]* and C. Merino[2]
[1]CENIM, Avda. Gregorio del Amo 8, E-28040 Madrid, Spain
[2]Werkstoffkunde und Werkstoffprüfung, Fachhochschule Gelsenkirchen, Germany

(Refereed)
(Received January 12, 1998; Accepted February 25, 1998)

ABSTRACT

Vapor grown carbon fibers (VGCFs) are the most promising potential substitutes for ex-PAN carbon fibers, because of their low cost. A standard tensile test for carbon fibers is not valid for several types of VGCFs because their thickness and very irregular morphology make it difficult to evaluate their equivalent diameter. After study of laser diffraction by Fourier transform, it is concluded that the diffraction patterns contain separate information about fiber diameter, in regular fibers, and fiber morphology. *© 1998 Elsevier Science Ltd*

KEYWORDS: A. composites, B. crystal growth, C. electron microscopy, D. defects

INTRODUCTION

Vapor grown carbon fibers (VGCFs) are produced by thermal decomposition of hydrocarbons in a hydrogen atmosphere in the presence of a metal catalyst [1–3]. Their low cost and easy production give VGCFs the capability of being used as inexpensive reinforcement in high performance composite applications [4]. Although up until now VGCFs have only been produced on a laboratory scale, research is being carried out to exploit their industrial potential. The final viability of these products depends on their industrial scale fabrication.

To compare VGCFs with ex-PAN and ex-Pitch fibers, tensile tests are widely used. Measurements for Young's modulus E, tensile strength σ, and failure strain ϵ involve the

*To whom correspondence should be addressed.

evaluation of the fiber diameter and the shape of the transverse section. For yarn or tow presented fibers, the thickness is easily calculated if density and length are known.

VGCFs are short fibers, from 1 mm up to 25 cm [5], with a wide range of thicknesses [6]. As in every duplex structure, their density [7] depends on the ratio between constituent phases, i.e., on the manufacturing process. As a consequence, the evaluation of a fiber section from density and fiber length data is not possible. In the present work, we compare the different techniques for determining fiber thickness presented in technical literature: optical projection microscopy [9,10], optical microscopy with an image analysis system [11], laser diffraction [12,13], and scanning electron microscopy (SEM) [14].

EXPERIMENTAL PROCEDURE

Sample Preparation. The samples used in this study were produced at 1,333 K, with a 70% H_2 + 30% CH_4 mixture as the precursor atmosphere. The thickness of the carbonaceous coating is controlled by selecting an appropriate process time: short processes produce thin fibers, longer processes yield thick fibers. If the process is excessively prolonged, the fibers become mostly pyrolytic carbon and are too weak.

To achieve a continuous sampling, a set of fibers were selected from different production profiles covering a wide range of thicknesses, from 4 to 12 μm. In the present work, two different types of generic fibers were chosen: F fibers were produced in a 25-min process (20 min for enlarging plus 5 min for thickening), while T fibers were manufactured in a 30-min process (20 and 10 min, respectively). Excessively thick fibers were avoided because they are difficult to handle. All samples were mounted in a Bristol paper frame, following ASTM D-3379.

The greatest difficulty of dry optical projection is focusing on a curled fiber. To solve this problem, dry and wet mountings were used. Dry mounting was achieved by placing the fiber between two glass slides. When wet mounting was used, the fiber was placed directly on a glass slide and immersed in a drop of Edmund Scientific Resolve immersion oil.

Thickness and Mechanical Properties Measurement. Conventional thickness measurement is designed for wholly cylindrical ex-PAN and ex-Pitch fibers with a diameter $\phi \geq 7$ μm. The morphology and thickness of VGCFs can have a much more complicated behavior than those of other types of fibers. Because in VGCFs, σ decreases very markedly with ϕ (achieving their optimal strength at $\phi = 5$ μm [8]), an accurate evaluation of their diameter is essential

For optical projection, fiber thicknesses were measured using a Zeiss Visopan optical 800× projector, according to ASTM D-3379–75. Optical image analysis was done using an Olympus Vanox AH3 optical microscope, with an Olympus Cue-2 image analyzer. The software of this system allows, in an easy way, many measurements *repeatedly on the same fiber*, to obtain a statistical evaluation of the error. SEM observations on VGCFs were made with a Jeol JXA 840 scanning electron microscope. For laser diffraction tests, an He–Ne Uniphase Novette 15082–2 laser (632.8 nm) was used with a 0.6 mm beam diameter at 0.5 mW.

A commercial MTS extensometer gauge was used in a tensile machine, with the samples clamped between a mobile screw and a digital Ametek Accuforce ML-4801–44 measurer. The screw scale allows elongations as low as 2 μm, and the force measurer has a full scale of 500 g, with a relative error of about 0.02%.

COMPARISON OF TECHNIQUES TO EVALUATE THE FIBER DIAMETER

Error Sources. From the definition of tensile strength σ

$$\sigma = \frac{4f}{\pi\phi^2} \tag{1}$$

the experimental error for σ and E modulus can be expressed as

$$\frac{\Delta\sigma}{\sigma} = \frac{\Delta f}{f} + 2\frac{\Delta\phi}{\phi} \tag{2}$$

$$\frac{\Delta E}{E} = \frac{\Delta\sigma}{\sigma} + \frac{\Delta\varepsilon}{\varepsilon} + \frac{\Delta l_0}{l_0} \tag{3}$$

where f is the rupture force, ϕ is the fiber diameter, l_o is the fiber length, and ε the failure strain.

In practical cases, for a typical VGCF sample with a 25 mm length and $\epsilon = 1.5\%$, the value of $\Delta\phi/\phi$ appears to be the most important statistical parameter. Image analysis can give a $\Delta\phi/\phi \approx 5\%$, which leads to a $\Delta E/E \approx 1\%$, clearly unacceptable for composite design.

The diffraction pattern is described in theory as the Fraunhofer diffraction through a cylindrical object. To obtain the experimental error, we used a standard error propagation, fixing $n = 1$, to get the maximum possible error. The resulting equation [12,13] is

$$\sin\alpha = \lambda/\phi \tag{4}$$

Differentiating and taking $d\gamma \cong 0$ ($d\gamma$ is really $\approx 10^{-2}$ nm according to the laser manufacturer specifications), we obtain

$$\frac{\Delta\phi}{\phi} = \frac{\lambda\cos\alpha}{\sin^2\alpha} \cdot \frac{1}{\phi} \cdot d\alpha \tag{5}$$

Using the simple trigonometric relation between α, a, and b, the final error expression can be rewritten as

$$\frac{\Delta\phi}{\phi} = A \cdot da + B \cdot db \tag{6}$$

where

$$A = \frac{b^2}{a(a^2 + b^2)} \tag{7}$$

$$B = \frac{b}{a^2 + b^2} \tag{8}$$

See appendix for further discussion of error sources in Fraunhofer diffraction.

Evaluation of the Diameter. In order to compare the accuracy of the four above-mentioned techniques for a wide range of fiber thicknesses, a systematic set of measurements was performed. A set of fibers was randomly chosen from several batches of our production. A

TABLE 1
Comparison of Results of Two Described Techniques, for the Same Fibers

	Diameter (μm)		
		Optical projection	
Sample	Laser diffraction	Dry	Wet
F_1	4.65 ± 0.01	4	4
T_1	8.23 ± 0.04	6	7

rough evaluation by dry-mounting optical projection allowed the collection of a set of fibers having different diameters, from 4 to 12 μm.

For a comparative test, two samples, F_1 and T_1, were measured by dry and wet optical projection and laser diffraction (Table 1). In comparison, optical projection microscopy yields thinner fibers than laser diffraction, hence gives an overestimation in fiber strength. If the fibers are thick, wet mounting gives more acceptable measurements than dry mounting, but, in any case, the error is remeasurable. In the case of very fine fibers, no influence of the mounting was observed, within measurement error.

Table 2 shows that the standard deviation for 70 fibers is distributed in seven sets. Maximal deviation corresponds to image analysis, and the minimal one corresponds to laser diffraction. For fibers having a similar diameter to commercial ex-PAN fibers, or medium thickness fibers, the difference between optical projection (wet) and laser diffraction was not significant. For thin fibers, the best technique was laser diffraction. For thick fibers in optical projection, there was a large difference between dry and wet mounting.

Finally, the previously measured VGCFs were examined by SEM. The thicknesses were evaluated on a graphic scale. The error depends on the many different parameters that define the electron microscope, intensity and accelerating voltage of the electron beam, distance from the sample to the detector, etc., besides the error of the graphic scale in the photos [14]. Differences between error sources were minimal for fibers of medium thickness. For very thick fibers, the difference was as much as 12%.

TABLE 2
Accuracy in % of Three Described Techniques on the Evaluation of Fiber Diameter for Different Ranges of Thickness

	Accuracy (%)			
			Optical projection	
Diameter (μm)	Laser diffraction	Image Analysis	Dry	Wet
$\phi < 6$	0.23	5.2	1.26	1.26
ϕ 6–8	0.41	2.1	1.20	0.42
$\phi > 8$	0.53	2.0	1.54	0.51

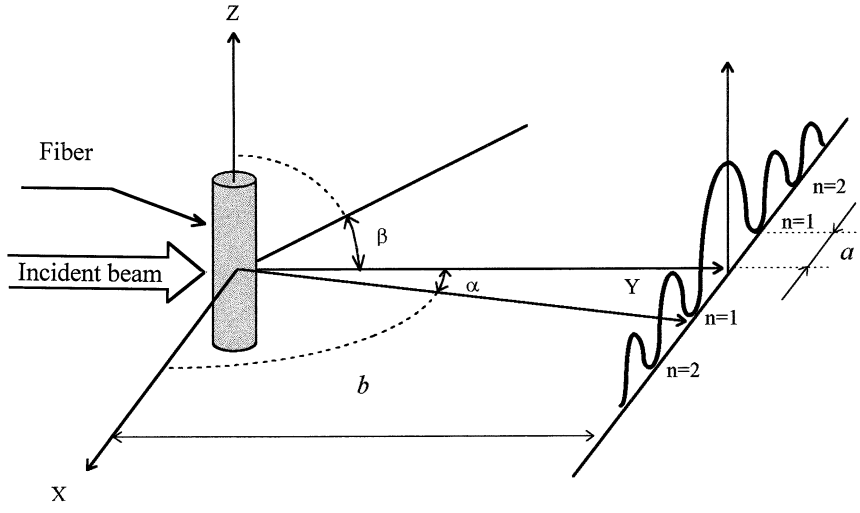

FIG. 1
Fraunhofer diffraction.

A comparison between laser diffraction and SEM measurements for a set of perfectly cylindrical samples is shown in ref. 14. The authors [14] obtained $d_{SEM} = d_{laser}$ for $\phi \cong 4.4$ μm; $d_{SEM} < d_{laser}$ for $\phi > 4.4$ μm, and $d_{SEM} > d_{laser}$ for (<4.4 μm. Due to the regularity of the samples used, a linear correlation was found [14] between both techniques,

$$d_{SEM}\ (\mu m) = 0.2805\ (\mu m) + 0.0367\ d_{laser}\ (\mu m) \tag{9}$$

with a coefficient of correlation equal to 0.9994. But, in irregular fibers, differences between SEM and laser measurements can be as much as ±20% [13].

EVALUATION OF MORPHOLOGICAL IRREGULARITIES

The use of Eq. 1 in Fraunhofer diffraction is only correct if we suppose that VGCFs are straight, perfect cylinders, which is not often the case. As an example, Figure 2 shows a set of seven fibers representative of the morphologies of VGCFs obtained in our laboratory in the last three years of work. For simplicity we have named them "perfect cylinder," "quasi-perfect cylinder," "cylinder with debris," "finely screwed thread," "palm tree trunk," "bar turned on a lathe" or "lathe shaped," and "crenulated" fibers.

Our procedure to grow VGCFs is described in ref. 15 and is basically an application of the method to grow whiskers developed by Wagner and Ellis [16] for metal microfilaments and used later by Portnoi et al. [17] to produce ceramic whiskers. Usually 90% of fibers per batch can be labeled as perfect cylinders and 10% must be considered as "quasi-perfect cylinders." The other morphologies are rare and only achieved with unusual and unadvisable operating conditions. When other routes are used to grow VGCFs [18], the other five types of fibers can be abundant.

Theoretical Diffraction Patterns. The diffraction process on a carbon fiber can be considered equivalent to the diffraction by a slit of width ϕ [20]. To obtain the characteristic

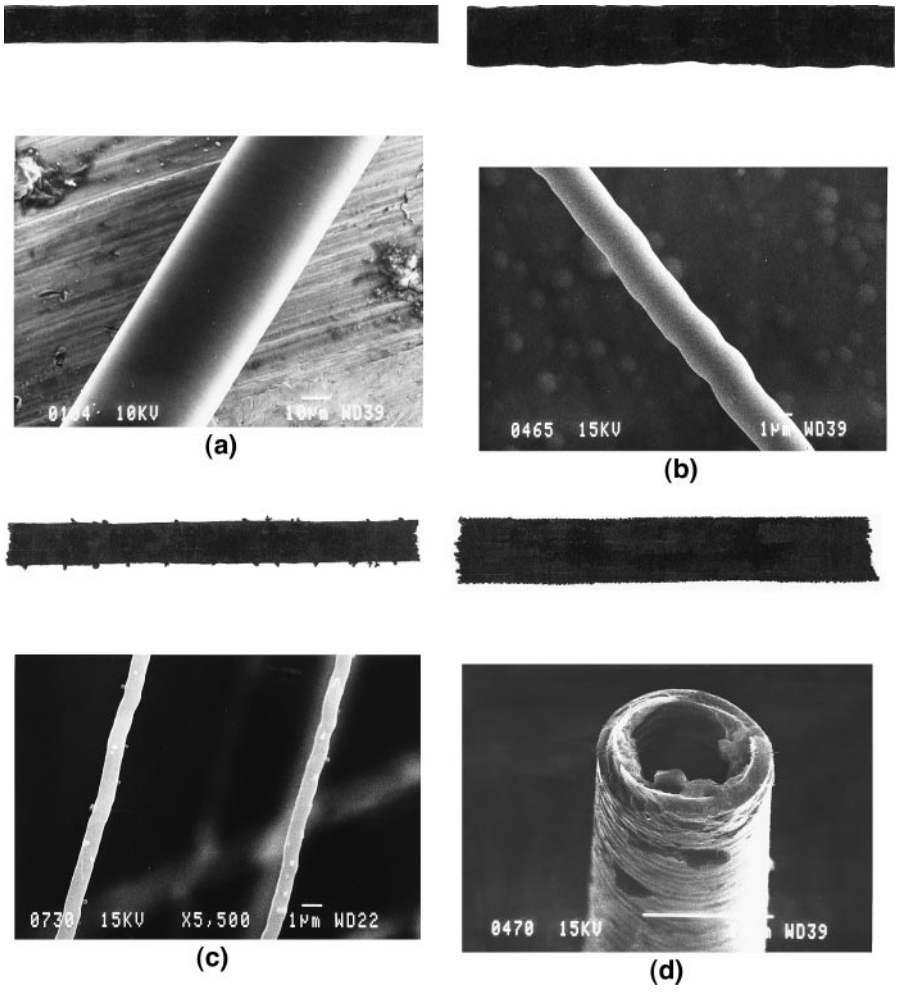

FIG. 2
Different morphologies in which VGCF can be grown: (a) perfect cylinder, (b) quasi-perfect cylinder, (c) cylinder with debris, (d) finely screwed thread, (e) palm tree trunk, (f) lathe shaped, and (g) crenulated.

patterns of each morphology, the profiles were digitized on an Epson GT-9000 scanner (see Figs. 2a–2g) and their Fourier transforms were calculated using a standard mathematical algorithm. Fourier transform for these profiles are represented in Figure 3. They are the laser diffraction patterns in "ideal conditions" (perfectly proportional darkening of the photographic film, no film absorption, etc.). If the object has only one symmetry axis, as in Figure 1, the Fourier transform will show only a pattern perpendicular to this axis. If there are several symmetry axes in the object, the Fourier transform will show a set of dotted rows perpendicular to each axis.

To observe this laser diffraction effect, a diffraction screen, as shown in Figure 4, is strongly recommended. The fiber can be observed throughout its length by moving it in perpendicular direction to the laser beam. When a local irregularity is in the beam, the *lost*

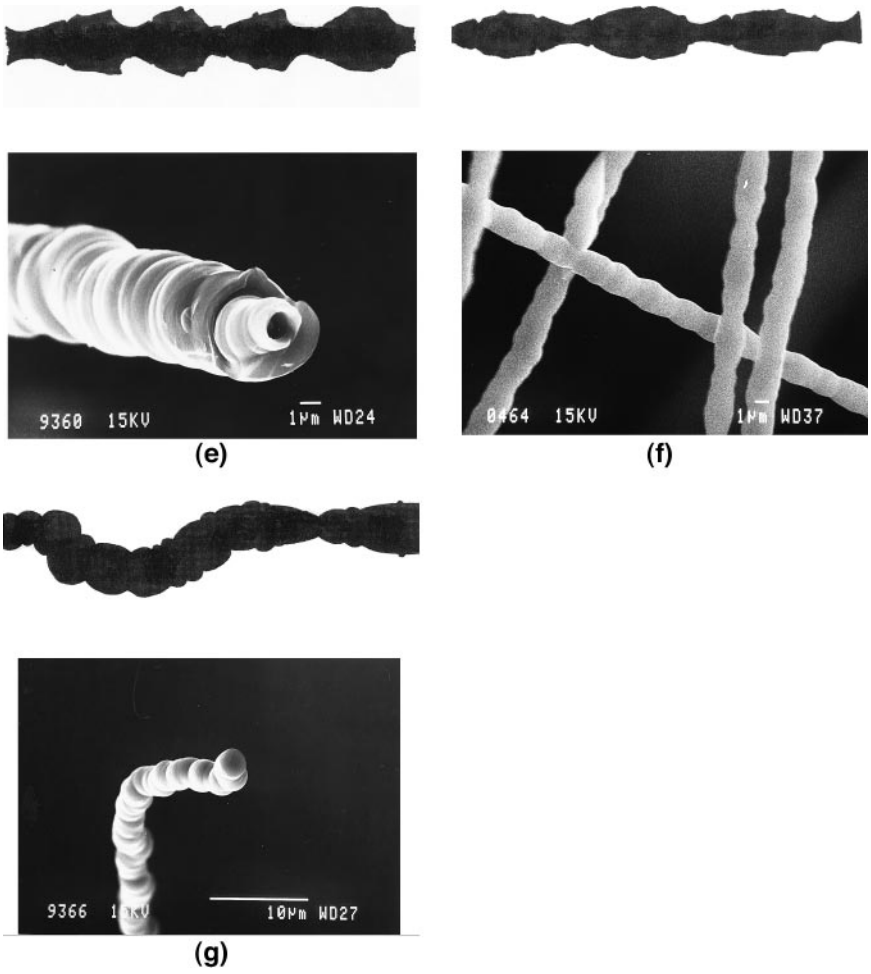

FIG. 2
Continued

center screen makes possible the observation of *satellite* lines without interference of the stronger central row pattern. In contrast, on the rear screen, the central row without satellite lines can be seen.

According to Figure 1, a single dotted row was expected to be found in Figure 3a. The parallel weak dots mean that the fibers shown in Figure 2a are not perfectly straight. This behavior can be explained because the melt drop mechanism starts from the beginning of the growing process at the base of the fiber [22]. Next to the tip of the fiber such coating is more recent and, consequently, because the cotical layer was less thick, the fiber section is smaller. Looking at very short distances, as given in Figure 2a, this soft cylindrical aspect is not recognizable. The laser diffraction beam covers 0.6 mm of the sample fiber length (laser beam diameter) that effectively crosses the beam. This distance corresponds to 120 diameters. In contrast, SEM values are averages of a small number of discrete diameters (4–5 times).

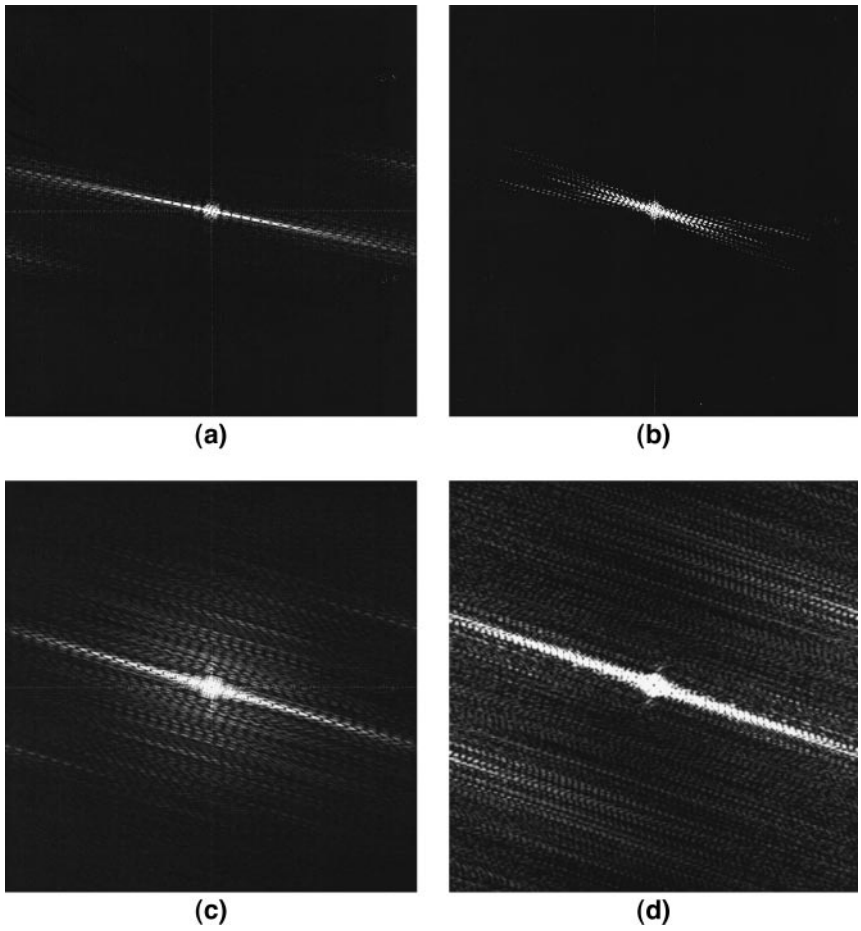

FIG. 3
Laser diffraction patterns of different VGCF outlines: (a) perfect cylinder, (b) quasi-perfect cylinder, (c) cylinder with debris, (d) finely screwed thread, (e) palm tree trunk, (f) lathe shaped, and (g) crenulated.

In the same way, we can explain the pattern shown in Figure 3b. In this case, the fiber presents a periodic change in diameter. This causes a periodicity in the direction perpendicular to the *z* axis, which results in the diffraction pattern being duplicated, triplicated, etc., on the *x* axis. The number of repetitions for distinct values of b depends on its frequency, that is, the number of times that the irregularity is repeated along a length of the fiber equal to the diameter of the laser beam.

$$\nu = D/\delta \tag{10}$$

where D is the diameter of the laser beam and δ is the distance between the consecutive irregularities. If the fiber had an elliptical cross section, we would have to rotate the fiber around its *z* axis in order to get the maximum and minimum values of ϕ, minor and major axes of the ellipse, respectively.

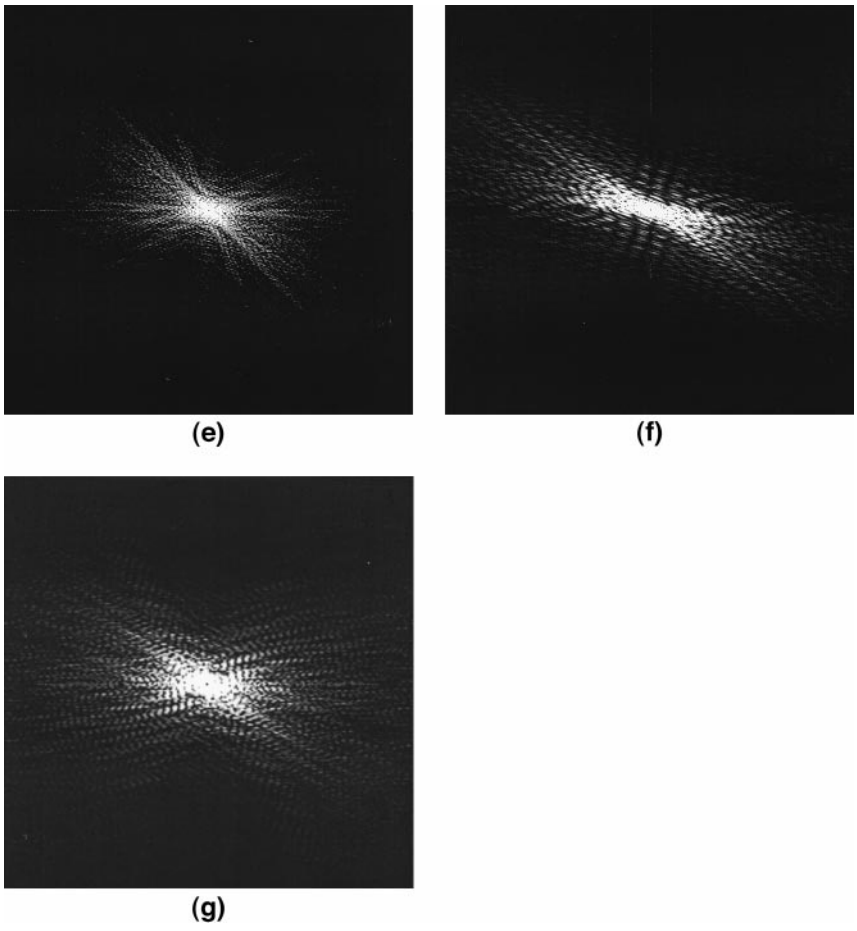

FIG. 3
Continued

The morphology named "cylinder with debris" (Fig. 2c) shows a cylinder with randomly distributed defects in the surface (influence on the Fourier image is negligible). However, Figure 3c shows abundant parallel satellites. These are due to the larger ratio between length and diameter (this is equivalent to saying that in Fig. 2c there are more waves). In the central row, the limit is clearly visible between two successive harmonics (gap between two neighboring dots). Hence, it is possible to calculate, with accuracy, the fiber equivalent thickness.

In Figure 2d, the *debris* is regularly located. Hence, the image of Figure 3d must be similar to Figure 3c (where L_2 is the continuation of L_1 and R_1 is prolonged by R_2). It is then possible to obtain a value for the equivalent thickness of the fiber.

The silhouette shown in Figure 2e can be idealized as a chain of identical isosceles trapeziums with the Fourier transforms similar to a Saint Andrew's cross. Figure 3e shows us a series of fuzzy crosses. Consequently, it is not possible to evaluate the equivalent thickness of the fiber using the central row.

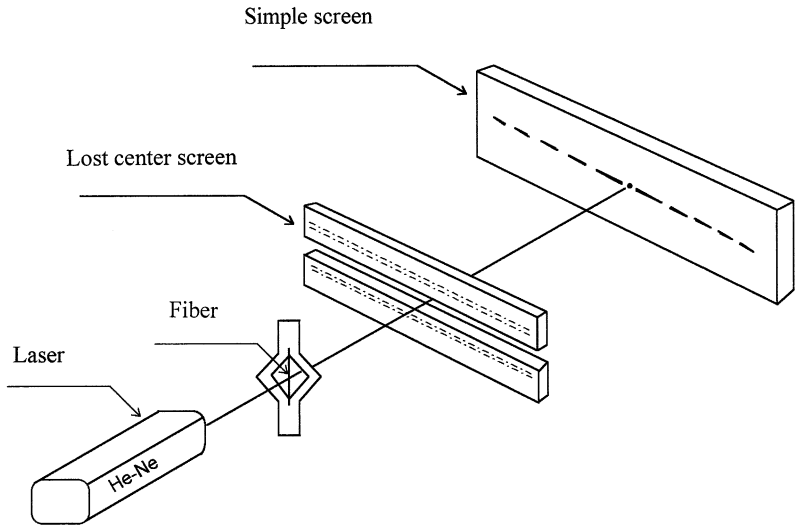

FIG. 4
Schematic representation of laser diffraction system.

Fiber morphology is equivalent in Figure 2f to the "palm tree trunk" type, but it is formed with differential segments randomly oriented, instead of finite segments. Figure 3f shows many differently oriented Saint Andrew's crosses. In this case, it is impossible to measure an equivalent thickness for the fiber.

Finally, crenulated fiber morphology is shown in Figure 2g. Since it is equivalent to a combination of particles forming a row, the diffraction image is equivalent to the pattern created by a nearly amorphous material, with a certain anisotropy (see Fig. 3g). In this case, it is impossible to measure the equivalent thickness of the fiber.

DISCUSSION

The main problem in the VGCFs tensile test is the previous measurement of their thickness. Because the standards for industrial fibers are prepared for straight and thicker filaments, they are not reliable for VGCF. As results are directly related to this parameter, it is interesting then to compare the error of each technique in the evaluation. However, the most widely used characterization technique for industrial fibers, optical microscopy, with or without image treatment, does not appear to be the best possible option. Other techniques such as SEM and laser diffraction could be valid.

With regard to the goal of measuring the diameter of the fiber, the use of laser diffraction is shown to be useful in the case where the fiber diameter is sufficiently uniform to qualify approximately as a cylinder. When the fiber diameter is subjected to more tortured geometries, values of mechanical properties obtained by tensile testing becomes questionable. Thus the laser diffraction method could be used to either measure the diameter or reject the fiber specimen from testing for mechanical properties.

In the area of crenulations and other defects, analysis of the fiber diameter by laser diffraction may be useful in determining statistical frequencies of selected defects, with the

goals of initially understanding the origin (largely unknown at present) of such defects and, ultimately, of eliminating them.

It is necessary then to interpret different VGCF patterns to understand the great advantages that laser diffraction offers. The lost center screen displays information concerning the defective morphology of each fiber as satellite lines. About fiber thickness, we can find enough information in the dotted row at the rear screen.

The similarity between a real diffractogram and the Fourier transform of a hypothetical fiber morphology, chosen among a set of morphologies of VGCFs, allows us to suppose a certain irregular morphology in the fiber, before single filament tensile test performance. In such cases, the sample is rejected and not tested. This procedure would be a precautionary measure that saves the performance of invalid tests in cases in which an unacceptable result would advise a further SEM exam of the broken fiber, to corroborate the regularity of the sample. This saves time and money that correspond with a SEM examination.

CONCLUSIONS

One of the problems with the engineering use of VGCFs is the variation of fiber properties resulting from various defects incorporated during synthesis of the fiber. This paper provides a method of determining the diameter, which is a necessary step in determining the mechanical properties of selected specimens.

VGCFs are subject to significant variations in fiber diameter, thus trying to determine the mechanical properties of these fibers by conventional tensile testing methods is problematic. The laser diffraction method we describe is a useful approach to measuring the diameter of such fibers. This method may also have merit in determining classes of defects which frequently appear in VGCFs, for example, the frequency of crenulations in the fiber.

Because it covers, with excellent accuracy, the range of the most frequent thicknesses, laser diffraction appears to be a powerful tool for performing an industrial evaluation of VGCFs. This is not an allowed tensile test under current standards for commercial ex-PAN or ex-Pitch fibers. Standards such as ASTM D-3379 could be amended in the future.

The study of the laser diffraction patterns gave us information which allowed us to place each sample in one of the following two categories:

1. *Regular fibers*. They have a good central pattern, with satellite parallel lines. An equivalent thickness, that could be valid to represent the mechanical strength of the filament, can be obtained for “perfect cylinder,” “quasi-perfect cylinder,” “cylinder with debris,” and “finely screwed thread” morphologies.
2. *Defective fibers*. They have a fuzzy central line with a complex satellite pattern, with no straight lines parallel to the central main row. Failure strength cannot be easily evaluated for “Palm trunk tree,” “lathe shaped,” and “crenulated” morphologies.

This precautionary technique of laser diffraction is recommended only for the peculiarities of VGCFs. In the case of commerically available cylindrical fibers, this precaution is not necessary; the standard procedure is adequate.

ACKNOWLEDGMENT

The present work was realized as an action of the Human Capital and Mobility Network (Contract CHRX-CT-94–0457). We thank the Commission of the European Communities for the financial help to perform this study.

APPENDIX

Error Sources in Fraunhofer Diffraction. The diffraction equation [12,13] is

$$\sin \alpha = n\lambda/\phi \tag{A1}$$

As our intention is to demonstrate that the accuracy of laser diffraction is better than the other three procedures to evaluate ϕ, we suppose $n = 1$. This means that we are using laser diffraction in a less favorable way, so we take

$$\sin \alpha = \lambda/\phi \tag{A2}$$

and differentiating we obtain

$$d\phi + \frac{1}{\sin \alpha} d\lambda + \lambda\left(\frac{-\cos \alpha}{\sin^2 \alpha}\right)d\alpha \tag{A3}$$

Since $d\gamma \cong 0$ ($d\gamma$ is really $\leq 10^{-2}$ nm, according to the laser manufacturer specifications), we can simplify this as

$$\frac{\Delta\phi}{\phi} = \frac{\lambda \cos \alpha}{\sin^2 \alpha} \cdot \frac{1}{\phi} \cdot d\alpha \tag{A4}$$

using Eq. A2 the result is

$$\frac{\delta\phi}{\phi} = \frac{\cos \alpha}{\sin \alpha} \cdot d\alpha \tag{A5}$$

In practice, α is evaluated by measuring a and b, according to Figure 1. So, Eq. A5 can be written as

$$\frac{\Delta\phi}{\phi} = \frac{b}{a} \cdot d\alpha \tag{A6}$$

and differentiating the simple trigonometric relation between α, a, and b, it is possible to obtain

$$d\alpha = \frac{b}{(a^2 + b^2)} da + \frac{a}{(a^2 + b^2)} db \tag{A7}$$

and by substitution of Eq. A7 into Eq. A6

$$\frac{\Delta\phi}{\phi} = \frac{b^2}{a(a^2 + b^2)} da + \frac{b}{a^2 + b^2} db \tag{A8}$$

Now, we define two homogeneous parameters,

$$A = \frac{b^2}{a(a^2 + b^2)} \text{ and } B = \frac{b}{(a^2 + b^2)} \tag{A9}$$

Then, we can finally write

$$\frac{\Delta\phi}{\phi} = A \cdot da + B \cdot db \tag{A10}$$

REFERENCES

1. G.G. Tibbetts, M. Endo, and C.P Beetz, *SAMPLE J.* **6**, 30 (1986).
2. F. Benissad, P. Gadelle, M. Couloun, and L. Bonnetain, *Carbon* **6**, 61 (l988).
3. F. Benissad, P. Gadelle, M. Couloun, and L. Bonnetain, *Carbon* **26**, 425 (1988).
4. G.P. Daumit, *Carbon* **27**, 759 (1989).
5. G.G. Tibbetts, *J. Crystal Growth* **73**, 431 (1985).
6. T. Koyama, *Carbon* **10**, 757 (1972).
7. G.G. Tibbetts, *Carbon* **27**, 745 (1989).
8. A. Madroñero, *Mater Sci. Eng., A* **105**, L1 (1994).
9. R. Moreton, *Fiber Sci. Technol.* **1**, 273 (1969).
10. H.W.M. Lunney, *Text. Res. J.* **50**, 728 (1980).
11. G.T. Vander Voort, *Int. Conf. Quantitative Microsc. Image Analysis* **21**, 19 (1993).
12. M. Koedam, *Philips Tech. Rev.* **27**, 208 (1966).
13. D.L. Dunaway, *J. Mater. Sci.* **30**, 4161 (1995).
14. C.T. Li and J.V. Tietz, *J. Mater. Sci.* **25**, 4694 (1990).
15. A. Madroñero, E. Ariza, and M. Verdu, *J. Mater. Chem.* **6**, 1059 (1996).
16. R.S. Wagner and W.C. Ellis, *Trans. Met. Soc. AIME* **233**, 1053 (1965).
17. K.Y. Portnoi, A.A. Mukaseev, V.N. Gribkov, A.S. Isaikin, and E.L. Umantsev, *Sov. Phys. Crystallogr.* **19**, 198 (1974).
18. P.A. Tesner, E.Y. Robinovich, I.S. Rafalkes, and E.F. Arefieva, *Carbon* **8**, 435 (1970).
19. W. S. Bickel, W. Gilliar, and B. Bell, *Appl. Opt.* **19**, 3671 (1980).
20. J. W. Goodman, *Introduction to Fourier Optics*, p. 62, McGraw-Hill, New York, (1968).
21. S. Hovmöller, *Microsc. Microanal. Microstruct.* **1**, 423 (1990).
22. A. Madroñero, *J. Mater. Sci.* **30**, 2061 (1995).